Title

TLR4 Signaling via NANOG Cooperates With STAT3 to Activate Twist1 and Promote Formation of Tumor-Initiating Stem-Like Cells in Livers of Mice

Journal

Gastroenterology, 150(3)

ISSN

0016-5085

Authors

Kumar, Dinesh Babu Uthaya

Chen, Chia-Lin

Liu, Jian-Chang

et al.

Publication Date

2016-03-01

DOI

10.1053/j.gastro.2015.11.002

Peer reviewed

Gastroenterology 2016;■:1–13

TLR4 Signaling via NANOG Cooperates With STAT3 to Activate *Twist1* and Promote Formation of Tumor-Initiating Stem-Like Cells in Livers of Mice

Q37 **Dinesh Babu Uthaya Kumar**,[1,*] **Chia-Lin Chen**,[1,*] Jian-Chang Liu,[1] Douglas E. Feldman,[2] Linda S. Sher,[3] Samuel French,[4] Joseph DiNorcia,[3] Samuel W. French,[5,6] Bita V. Naini,[5] Sunhawit Junrungsee,[7] Vatche Garen Agopian,[7] Ali Zarrinpar,[7] and Keigo Machida[1,8]

[1]Department of Molecular Microbiology and Immunology, [2]Department of Pathology, [3]Department of Surgery, Keck School of Medicine of University of Southern California, Los Angeles, California; [4]Department of Pathology, Harbor-University California Los Angeles Medical Center, [5]Department of Pathology and Laboratory Medicine, [6]Jonsson Comprehensive Cancer Center University of California Los Angeles, [7]Department of Surgery, University of California Los Angeles School of Medicine,
Q3 Q4 *[8]Southern California Research Center for ALPD and Cirrhosis*

BACKGROUND & AIMS: Obesity and alcohol consumption contribute to steatohepatitis, which increases the risk for hepatitis C virus (HCV)-associated hepatocellular carcinomas (HCCs). Mouse hepatocytes that express HCV-NS5A in liver upregulate the expression of Toll-like receptor 4 (TLR4), and develop liver tumors containing tumor-initiating stem-like cells (TICs) that express NANOG. We investigated whether the TLR4 signals to NANOG to promote the development of TICs and tumorigenesis in mice placed on a Western diet high in cholesterol and saturated fat (HCFD). **METHODS:** We expressed HCV-NS5A from a transgene (NS5A Tg) in *Tlr4*-/- (C57Bl6/10ScN), and wild-type control mice. Mice were fed a HCFD for 12 months. TICs were identified and isolated based on being CD133+, CD49f+, and CD45-. We obtained 142 paraffin-embedded sections of different stage HCCs and adjacent nontumor areas from the same patients, and performed gene expression, immunofluorescence, and immunohistochemical analyses. **RESULTS:** A higher proportion of NS5A Tg mice developed liver tumors (39%) than mice that did not express HCV NS5A after the HCFD (6%); only 9% of *Tlr4*-/- NS5A Tg mice fed HCFD developed liver tumors. Livers from NS5A Tg mice fed the HCFD had increased levels of TLR4, NANOG, phosphorylated signal transducer and activator of transcription (pSTAT3), and TWIST1 proteins, and increases in *Tlr4*, *Nanog*, *Stat3*, and *Twist1* messenger RNAs. In TICs from NS5A Tg mice, NANOG and pSTAT3 directly interact to activate expression of *Twist1*. Levels of TLR4, NANOG, pSTAT3, and TWIST were increased in HCC compared with nontumor tissues from patients. **CONCLUSIONS:** HCFD and HCV-NS5A together stimulated
Q10 TLR4-NANOG and the OB-R-pSTAT3 signaling pathways, resulting in liver tumorigenesis through an exaggerated mesenchymal phenotype with prominent *Twist1*-expressing TICs.

Keywords: HCC; HCV; Obesity; NASH.

Q11 Q12 Q13 Obesity and infection by hepatitis C virus (HCV) are connected pathophysiologically to hepatocarcinogenesis.[1–5] The risk for hepatocellular carcinoma (HCC) increases from 8.6-fold to 47.8-fold as a result of concomitant obesity in HCV-infected patients.[4] Obesity
Q14 induced by a high-cholesterol high-fat diet (HCFD) is associated with increased levels of serum bacterial endotoxin derived from the hepatic portal and/or the systemic gut; these increased levels stimulate the expression of proinflammatory cytokines in the liver and adipose tissues, subsequently leading to liver injury.[5–7] Such HCFD-mediated changes superimposed on HCV infection lead to an increased incidence of overt diabetes,[8] potentially establishing a self-reinforcing oncogenic cycle.

HCC, the fifth most common cancer in the world and the third leading cause of cancer mortality, has a low 5-year survival rate because of a lack of effective therapeutic options.[9,10] An understanding of the molecular mechanisms of hepatocarcinogenesis will be required for the development of improved therapeutic models for this disease. The HCV-NS5A protein, a major target of therapeutic efforts, suppresses activity of interferon-induced, double-stranded, RNA-activated protein kinase PKR,[11] accounting for the resistance of most HCV strains to interferon treatment. Furthermore, NS5A transactivates many gene promoters.[12] We recently showed that HCV infection and the associated expression of the NS5A protein lead to excessive tumor necrosis factor α production, fulminant hepatitis, and a 6-fold increase in mortality in response to gram-negative bacterial-derived lipopolysaccharide (LPS) ligand.[13] These effects are mediated through increased expression of the innate immune receptor Toll-like receptor 4 (TLR4), a transmembrane receptor that activates nuclear factor-κB and induces a proinflammatory and tumorigenic gene

Q15

BASIC AND TRANSLATIONAL LIVER

*Authors share co-first authorship.

Abbreviations used in this paper: **AFP, _____; ChIP, chromatin immunoprecipitation; EMT, epithelial mesenchymal transition; HCC, hepatocellular carcinoma; HCFD, high-cholesterol fat diet; HCV, hepatitis C virus; LFD, low-fat diet; LPS, lipopolysaccharide; mRNA, messenger RNA; OB-R, _____; PCR, polymerase chain reaction; pSTAT3, phosphorylated signal transducer and activator of transcription 3; shRNA, short hairpin RNA; Tg, transgene; TICs, tumor-initiating stem-like cells; TLR4, Toll-like receptor 4; TSS, transcription initiation/start site; USC, _____; WT, wild-type.**

0016-5085/$36.00
http://dx.doi.org/10.1053/j.gastro.2015.11.002

Q1 expression program in HCV-infected livers. Likewise, increased TLR4 signaling in NS5A-positive hepatocytes after chronic and excessive alcohol consumption promotes the expansion of highly malignant, $CD133^{+}/CD49f^{+}/Nanog^{+}$ liver tumor-initiating stem-like cells (TICs) in alcohol-associated hepatocarcinogenesis.[14] Nevertheless, the significance of TLR4 in hepatocarcinogenesis associated with obesity and HCV infection and the role of proteins involved

A

Disruption of *Tlr4* reduces tumor development in HCV *NS5A*Tg mice fed HCFD or LFD for 12 months

	Diet	N	Tumor Incidence (%)	Survival (%)	Body weight Begin (g)	Body weight End (g)	Ratio of liver/body (%)
Wild type	LFD	22	0	95	21.8 ± 3.8	33.6 ± 3.5	4.6
Tlr4-/-	LFD	33	0 ns	94 ns	20.1 ± 2.9	31.9 ± 2.8	4.2
*NS5A*Tg	LFD	23	0 ns	91 ns	21.9 ± 3.7	32.5 ± 3.9	4.2
Tlr4-/- *NS5A*	LFD	19	0 ns	89 ns	20.2 ± 3.2	32.3 ± 2.7	4.2
Wild type	HCFD	20	6 ns	90 ns	20.9 ± 2.6	42.9 ± 5.5	3.9
Tlr4-/-	HCFD	20	0 ns/ns	90 ns/ns	20.4 ± 3.3	34.2 ± 4.2***	4.4
*NS5A*Tg	HCFD	40	39***/**	78 ns/ns	20.2 ± 2.7	45.5 ± 6.2	5.7 *
Tlr4-/- *NS5A*	HCFD	38	9 ns/ns	84 ns/ns	20.7 ± 3.8	36.5 ± 4.6***	4.5
Wild type	LPS + HCFD	20	6 ns/ns	95 ns/ns	20.6 ± 2.8	38.2 ± 4.5	5.0
Tlr4-/-	LPS+ HCFD	17	0 ns/ns	90 ns/ns	21.1 ± 2.3	32.6 ± 3.8*	4.4
*NS5A*Tg	LPS+ HCFD	21	47 ***/ns	81 ns/ns	20.8 ± 3.1	37.1 ± 3.8	7.8 **
Tlr4-/- *NS5A*	LPS+ HCFD	19	13 ns/**	84 ns/ns	20.1 ± 3.9	32.2 ± 3.3*	4.7

B

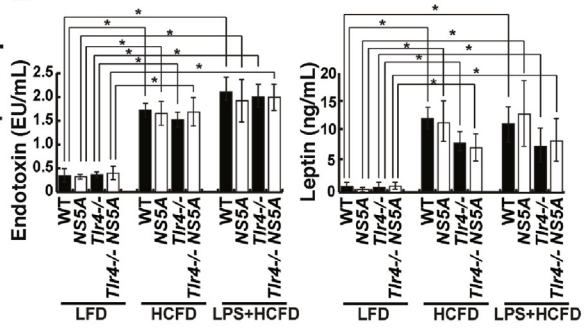

C

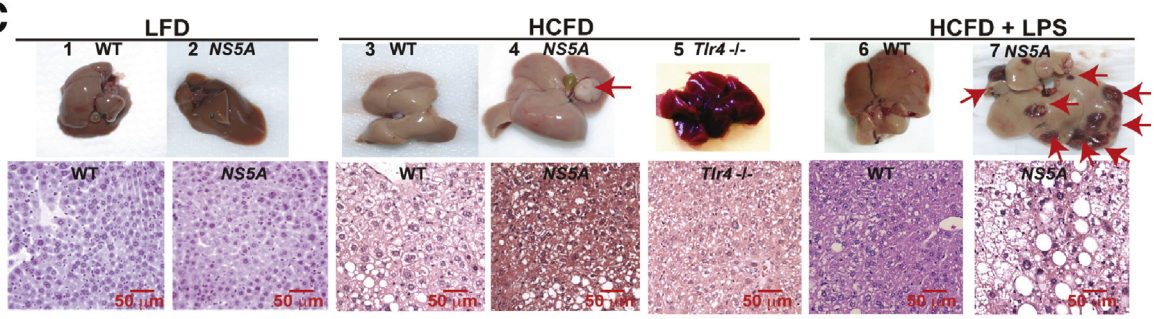

D

Histology	WT Dysplastic nodule	WT HCC	*NS5A* Dysplastic nodule	*NS5A* HCC
LFD	0/21 (0%)	0/21 (0%)	0/21 (0%)	0/21 (0%)
HCFD	1/18 (5.6%)	0/18 (0%)	8/31 (25.8%)	4/31 (12.9%)
LPS + HCFD	1/19 (5.3%)	0/19 (0%)	4/17 (23.5%)	4/17 (23.5%)

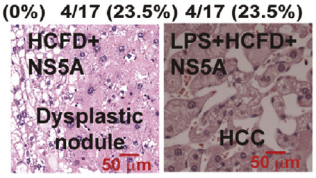

E

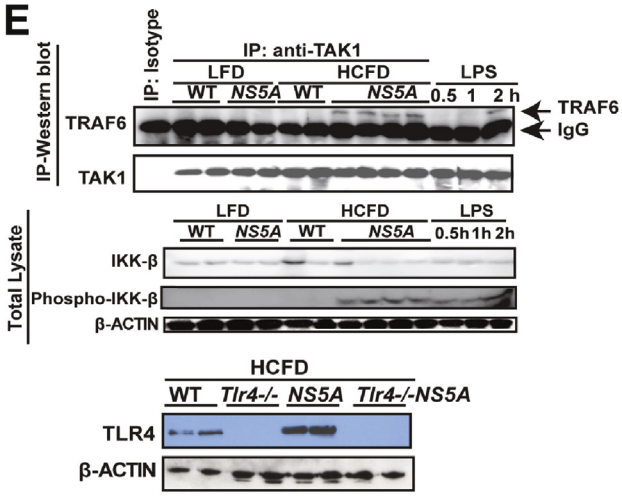

F

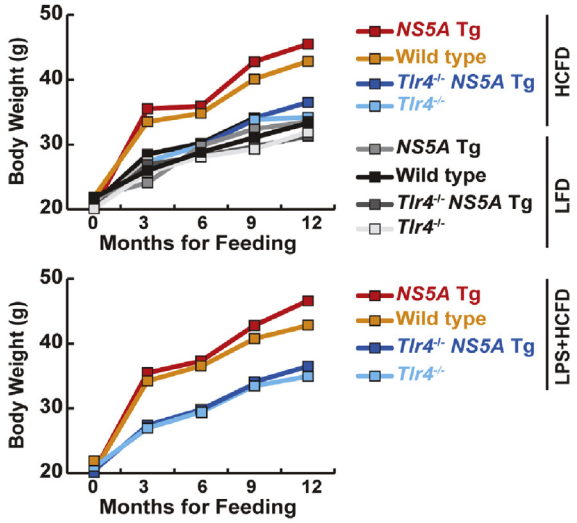

in the metastatic properties of TICs has not been addressed directly.

Long-term consumption of a HCFD increases levels of gut-derived bacterial endotoxin in the plasma.[15] We previously showed increased expression of TLR4 (a receptor for endotoxin) in hepatocytes of NS5A-transgene (Tg) mice.[14] Based on these findings, we postulated that synergism between HCV and obesity in liver disease progression involved TLR4-dependent signaling. We also reasoned that the TLR4-NANOG Q16 pathway might play a major role in mediating the synergism between obesity and HCV in the pathogenesis of HCC via generation of $CD133^+/Nanog^+$ TICs. Our RNA microarray analysis on TICs derived from HCFD fed mice showed a significant increase in *Twist1*. We previously showed that leptin and its receptor (OB-R) augmented phosphorylated signal transducer and activator of transcription 3 (pSTAT3) in TICs,[16] these results led us to hypothesize that adipose tissue-derived leptin-pSTAT3 and TLR4-NANOG signals are needed for activation of *Twist1* in TICs. Here, we provide evidence that TLR4 drives oncogenesis in part through the transcriptional induction of *Twist1*, a master regulator of epithelial mesenchymal transition (EMT),[17–19] to generate cells with stem-like properties and a predisposition to the EMT. This signaling module therefore represents a new candidate target in the treatment of obesity- and HCV-associated HCC.

Materials and Methods Q17

Additional details are described in the Supplementary Materials and Methods section and in Supplementary Tables 3–6.

Mouse Studies

Q18 All experiments on mice were approved by the USC Institutional Animal Care and Use Committee. Transgenic mice Q19 Q20 expressing the HCV-NS5A gene under control of the *Apo*E promoter[20,21] were obtained from Professor Ratna Ray (Saint Louis University, St. Louis, MO). TLR4-deficient mice (C57Bl6/10ScN), control mice (C57Bl6/10ScSn), and C57Bl/6 mice were Q21 purchased from Jackson Laboratories. To generate wild-type (WT), NS5A, *Tlr4*-/-, and *Tlr4*-/-NS5A mice on a more congenic genetic background, NS5A Tg (FVB strain) and Tlr4-/- mice were cross-bred on a C57BL/6 background (Jackson Laboratories) for more than 8 generations at USC. Littermates on mixed C57BL/6-NS5A transgenic and *Tlr4*-/- mice (Jackson Laboratories) were intercrossed for at least 8 generations to produce WT, NS5A, *Tlr4*-/-, and *Tlr4*-/-NS5A mice on a more congenic genetic background. Both sexes of mice were used for experiments. The HCFD diet was modified from TD.03350 (Harkan Teklad, Inc) as previously described.[22,23] Where indi- Q22 cated, mice were fed ad libitum with an ethanol-containing Lieber-DeCarli diet containing 3.5% ethanol or isocaloric dextrin (Bioserv, Frenchtown, NJ) HCFD beginning at 8 weeks of age for a period of 12 months. Other mice were fed modified high-fat AIN-93G purified ethanol liquid diet with anhydrous milk fat, lard, corn oil, and 1% cholesterol (DYET 710362; Dyets, Inc) or Lieber-DeCarli Regular Control Diet (DYET 710027).

Human Subjects

Paraffin-embedded tissue sections were obtained in accordance with the approved Institutional Review Board. There were 3 institutions (University of Southern California, University of California at Los Angeles, and University of Minnesota) that granted Institutional Review Board approval for the supplied specimens. Specimens were obtained from the Liver Tissue Cell Distribution System at the University of Minnesota according to the following criteria: surgically excised HCC tissues from 8 patients ± HCV infection, ± history of alcoholism, ± obesity/diabetes/body mass index greater than 30. Eighteen specimens also were obtained from the Hepatobiliary and Liver Transplantation Service at the USC Keck School of Medicine. A total of 116 cases of HCC were identified from 2002 to 2011 by searching the University of California at Los Angeles Department of Pathology database using the following search terms: liver, hepatocellular carcinoma, resection, and transplant. All patient identifiers were removed to protect confidentiality. Samples were obtained from both sexes between the ages of 42 and 80. Histologically, all samples showed varying degrees of microvesicular and macrovesicular steatosis and inflammation in addition to different stages of HCC. These paired 116 specimens were the livers that had been dissected with the tumor

Figure 1. NS5A Tg mice fed HCFD with or without LPS frequently developed tumors. (*A*) Summary of WT and *Tlr4*$^{-/-}$ HCV-NS5A Tg mice fed control diet or HCFD with or without LPS from 8 weeks of age for 12 months. N, number of experimental mice. WT-HCFD; $*P < .05$ $**P < .01$ $***P < .005$, green scripts and symbols, statistical analysis in comparison with LFD; purple scripts and symbols, statistical analysis in comparison with HCFD. (*B*) Plasma endotoxin and leptin levels in mice fed LFD or HCFD. (*C*) Gross images of nonpathologic liver from control diet (1, 2) and liver tumor with multiple nodules from HCFD (3–6) and HCFD + LPS (7). *Lower panel*: Histology of respective groups. The HCFD tumor shown (*arrow*) is a dysplastic nodule. (*D*) Frequencies of liver dysplastic nodules and HCCs in LFD– or HCFD–WT or NS5A Tg mice fed LFD or HCFD for 12 months. Representative H&E staining of tumor sections from WT or NS5A Tg mice fed HCFD or LPS + HCFD. The histopathology of the tumors (*arrows*) shown are dysplastic nodules or HCCs based on their hypercellularity. Nodular lesions differ from the surrounding liver parenchyma with cytologic or structural atypia. (*E*) Normal liver/liver tumor lysates from WT and NS5A Tg mice fed control chow or HCFD were analyzed for LPS-induced TLR4 signaling. *Upper panel*: Tumor necrosis factor–receptor–associated factor 6 (TRAF6) interaction with transforming growth factor α–activated kinase 1 (TAK1), was enhanced in NS5A Tg mice fed HCFD. The interaction between TAK1 and TRAF6 was examined by immunoblots after immunoprecipitation (IP) with TAK1 antibody. As a positive control (shown in last 3 lanes), mice were challenged with LPS; LPS was injected (2 mg/kg) 30 minutes, 1 hour, or 2 hours, respectively, before liver tissues were collected for analysis. The relative densitometry units and details are available in Supplementary Figure 1*A*. *Bottom panel*: LPS-induced phosphorylation of IKK-β in the liver was increased in NS5A Tg mice fed HCFD. Positive controls (last 3 lanes), as explained previously. (*F*) Data summary of body weight changes over a 12-month feeding period and statistics are available in panel *A*. *Scale bar*: 50 μm.

and adjacent noncancerous areas from the same patients. Clinicopathologic information is described in Supplementary Figure 10 and summarized in Supplementary Table 1.

Results

HCFD Promotes Liver Oncogenesis in NS5A Tg Mice in a TLR4-Dependent Manner

We used an in vivo loss-of-function strategy to test the role of TLR4 in this interplay between NS5A and obesity. Hepatocyte-specific NS5A Tg,[20,21] and WT mice with or without TLR4 deficiency (*Tlr4*$^{-/-}$)[14] were maintained on a low-fat diet (LFD) or an HCFD with or without supplemental LPS for 12 months (Figure 1*A*). HCFD consumption resulted in an obese population (WT and NS5A Tg mice); however, this outcome remarkably was prevented by TLR4 deficiency in either genotype (Figure 1*A* and *F*). In HCFD mice, we observed a liver tumor incidence of 39% in NS5A Tg mice compared with 6% in WT mice. By contrast, we observed a significant decrease of tumor incidence to 9% in *Tlr4*$^{-/-}$NS5A Tg mice (Figure 1*A* and *C*). Conversely, LPS supplementation in the HCFD (100 mg/kg) further increased the incidence to 47% in NS5A Tg mice (Figure 1*A*). This observation indicated a significant contribution of the LPS-TLR4 pathway in hepatocarcinogenesis. In addition, the presence of NS5A in HCFD-fed mice significantly increased the liver to body ratio, which coincided with severe liver hepatomegaly and inflammation (Figure 1*A* and *C* and Supplementary Table 2).

As predicted, HCFD, and HCFD + LPS feeding markedly increased plasma endotoxin and leptin levels in all tested cohorts (Figure 1*B*). Several liver malignancies were observed in *NS5A Tg* mice, but not in the control animals. Additional observed pathologies included nonalcoholic steatohepatitis–like bloating (Figure 1*C*), dysplastic nodules (nonmalignant), and HCCs (Figure 1*D*). Activation of TLR4 signaling was assessed by co-immunoprecipitation of transforming growth factor α–activated kinase 1–tumor necrosis factor receptor–associated factor 6, and immunoblotting for p-IKK-β.[14] Concomitant TLR4 activation through tumor necrosis factor receptor–associated factor 6–transforming growth factor α–activated kinase 1–p-IKK-β was evident in HCFD-fed NS5A Tg (Figure 1*E*, and Supplementary Figure 1), but not in LFD-fed cohorts. As a positive control for TLR4 activation parameters, a single intraperitoneal dose of LPS (2 mg/kg) was given to chow-fed WT mice before sample collection (last 3 lanes of Figure 1*E*, top). Collectively, these results showed that HCV-NS5A and HCFD acted synergistically to induce liver tumors in a manner dependent on TLR4.

Twist1 *Identified as one of the Most Conspicuously Up-Regulated Genes in TLR4-Dependent NS5A- and HCFD-Driven Hepatocarcinogenesis*

To understand the molecular basis of enhanced liver oncogenesis in HCFD-NS5A mice, we performed RNA microarray analysis. This identified 131 differentially up-regulated and 43 down-regulated transcripts in HCFD-fed NS5A Tg mice (Figure 2*A* and Supplementary Figure 2). Some of the more highly up-regulated transcripts of different functional categories are listed in Figure 2*A*. These include the stemness marker *Nanog*, oncogene *Igf2bp3*, and EMT and tumor metastasis regulator *Twist1*.[19,24,25] *Nanog* and *Igf2bp3* have been found to be critical in self-renewal and tumorigenic activity of TICs isolated from liver tumors of alcohol-fed NS5A mice.[14] To confirm that TLR4 activation in the liver is from TICs, we performed immunofluorescence staining on control, HCFD, and HCFD + LPS livers (Supplementary Figure 3). This analysis confirmed that the source of TLR4 in the HCFD and HCFD + LFD livers is from TICs (TLR4 co-staining with NANOG) and not from the resident macrophages (Kupffer cells). For this study, we further examined the molecular mechanisms through which *Twist1* promoted EMT and tumor metastasis in HCFD-fed NS5A-derived TICs. To substantiate the microarray data we performed quantitative real-time polymerase chain reaction (PCR) analysis to measure *Twist1* gene expression. As expected, *Twist1* messenger RNA (mRNA) was induced significantly in HCFD-fed NS5A Tg mice compared with HCFD-fed WT mice or LFD-fed NS5A Tg mice (Figure 2*B*). These analyses also showed that *Twist1* transcription was reduced in the HCFD-fed *Tlr4*$^{-/-}$ NS5A Tg cohort (Figure 2*B*), suggesting that the presence of TLR4 was permissive or required for *Twist1* induction.

TLR4 Signaling Transactivates Twist1

To further establish whether TLR4 regulates *TWIST1*, human HCC cell line Huh7 cells were transfected with the NS5A gene expression vector. We then transduced lentivirus expressing *TLR4* or scrambled short hairpin RNA (shRNA) in these NS5A/vector-expressing cells and further stimulated these cells with or without LPS. As shown in Figure 2*C*, LPS treatment up-regulated *TWIST1* mRNA levels in NS5A-transfected Huh7 cells transduced with scrambled shRNA, but not in any other groups with shRNA knockdown of TLR4. *TWIST1* induction was abrogated significantly by TLR4 blockade. When a dominant-negative variant of TLR4 lacking the cytoplasmic domain (mutant TLR4; TLR4ΔCyt) was transduced into these cells, a similar and more conspicuous reduction of *TWIST1* expression was observed. We then tested whether TLR4 signaling can transcriptionally activate *TWIST1*. Huh7 cells were transfected with *TWIST1* promoter (nt -700/-1) luciferase plasmid constructs[26] and assayed for activity upon LPS treatment. A potent *TWIST1* promoter activity was observed that was responsive to the LPS-TLR4 signaling axis (Figure 2*D*), indicating that TLR4 does indeed transactivate *TWIST1*.

Twist1 *Blockade Reduces TIC Self-Renewal, Migration, and Tumorigenesis*

To show that TLR4 is responsible for *Twist1* induction in TICs, we isolated CD133+/CD49f+/CD45- cells for examination of gene expression to show that these cells indeed express higher levels of stemness genes and *Twist1* (Figure 3*A*). The functionality of *Twist1* in TICs was analyzed by silencing expression using lentivirus expressing *Twist1* shRNA. *Twist1* silencing did not affect TLR4 or

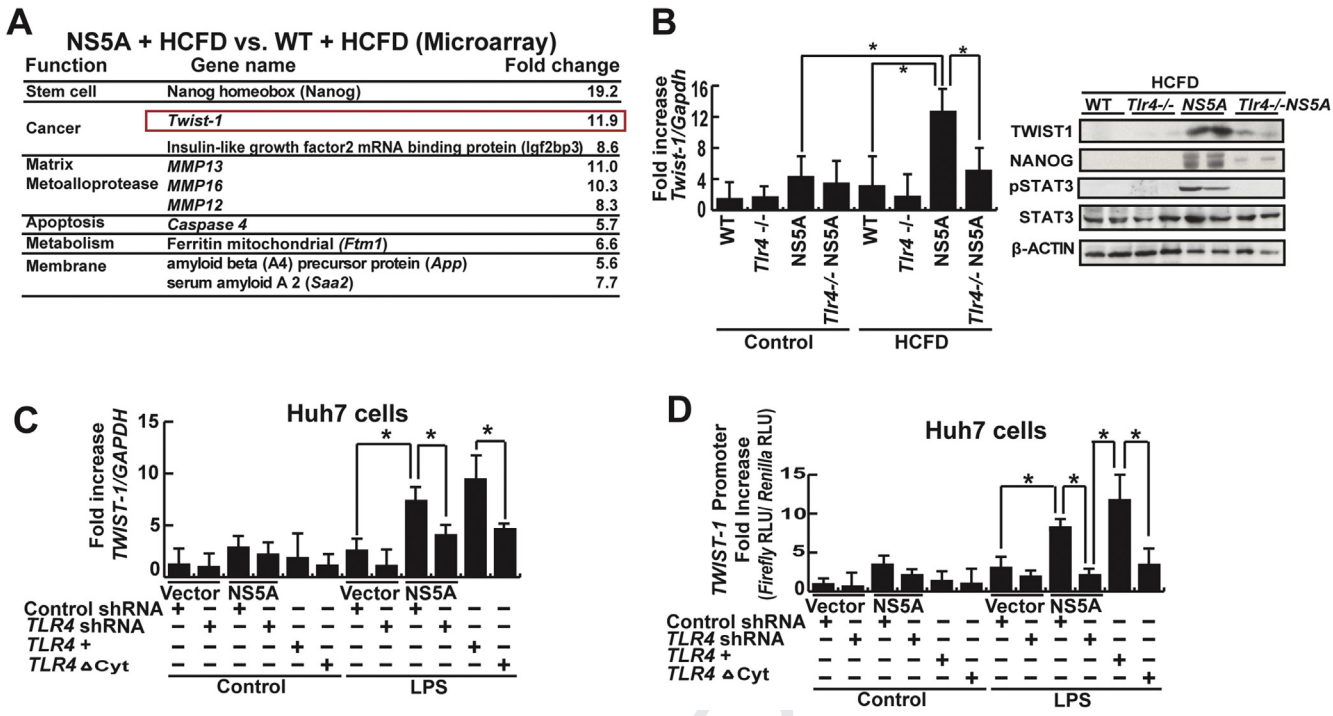

Figure 2. TLR4-mediated TWIST1 induction. (*A*) Chief summary of RNA microarray analysis. *Twist1*, a key regulator of EMT signaling, was significantly higher in NS5A + HCFD compared with WT + HCFD. (*B*) Quantitative analysis of *Twist1* from liver/liver tumor tissues of all cohorts, as listed in Figure 1*A*. Heightened *Twist1* expression (NS5A Tg mice fed HCFD) was abrogated by TLR4 deficiency. Data normalized to glyceraldehyde-3-phosphate dehydrogenase expression are listed as the fold-change (*$P < .05$). (*C*) LPS induced *TWIST1* in Huh7 cells transduced with an NS5A expression vector (*$P < .05$ compared with cells transduced with an empty vector). This was suppressed by lentiviral expression of shRNA for *TLR4* and also in cells transduced with the dominant-negative TLR4 vector (TLR4ΔCyt). (*D*) LPS induced *TWIST1* promoter activity. Huh7 cells transfected with *TWIST1* promoter-luciferase construct were stimulated with LPS (10 μg/mL) in culture. Other experimental procedures in this figure are the same as described earlier. TLR4 knockdown or mutation abrogated *TWIST1* promoter activity, but adding TLR4 rescued it. Relative light unit (RLU) values were normalized by the *Renilla* luciferase activity driven by the SV40 promoter, which were used as a transfection control (*$P < .05$).

NANOG (downstream of the LPS-TLR4 axis[14]) protein expression (Figure 3*B*), but up-regulated epithelial cell markers *albumin* and *E-cadherin* expression while down-regulating expression of a mesenchymal cell marker, *N-cadherin* (Figure 3*C*); thus indicating that *Twist1* silencing changes the mesenchymal phenotype to the epithelial phenotype. These data indicated that *Twist1* acts downstream of the TLR4 signaling cascade and contributes significantly to the maintenance of mesenchymal phenotype based on its effect on *albumin*, *E-cadherin*, and *N-cadherin*. To further investigate this phenomenon, we assessed the phenotypic changes in TICs after *Twist1* blockade. TIC morphology was altered from a spindle (mesenchymal) shape to a tadpole-like (epithelial) shape (Figure 3*D*, inset); there also was increased cell size (Supplementary Figure 4*A*). Moreover, *Twist1* blockade significantly reduced cell proliferation (Supplementary Figure 4*B*), self-renewal ability as assayed by colony formation in soft agar (Figure 3*D*), spheroid formation (Supplementary Figure 4*C*), and cell migration by scratch assay (Figure 3*E*). We then tested implanted cells for tumorigenic potential in NOG mice. Subcutaneously transplanted *Twist1* or scrambled shRNA TICs were monitored for tumor size over a period of 35 days. Gross and optical image analysis of live tumor-bearing mice showed reduced tumor size in *Twist1* knockdown groups (Figure 3*F*, panels 3 and 4). As expected, tumor volume and weight were reduced significantly (Figure 3*F*, panels 1 and 2). Histologic examination of xenografted TICs showed that the resulting tumor showed HCC morphology (Figure 3*F*, panel 5). These results showed that *Twist1*, regulated through the LPS–TLR4 axis, plays a significant role in maintaining the mesenchymal and tumorigenic properties of TICs.

NANOG and pSTAT3 Regulate Twist1

We next investigated the molecular mechanisms responsible for TLR4-dependent activation of *Twist1*. We performed *Twist1* promoter-reporter assays, using promoter constructs[26] containing either WT (nt -700 to -1) or mutated regions upstream of the transcription initiation/start site (TSS). The activation of these reporter constructs was analyzed in cells transduced with either scrambled or *Tlr4* shRNA. From this analysis we established that the region between -209 to -51 is essential for the basal and *Tlr4*-dependent induction of *Twist1* in TICs (Figure 4*A* and Supplementary Figure 5, Huh7 cells). In particular, a deletion between nts -102 and -74 markedly reduced *Twist1* promoter activity, indicating that this region contained

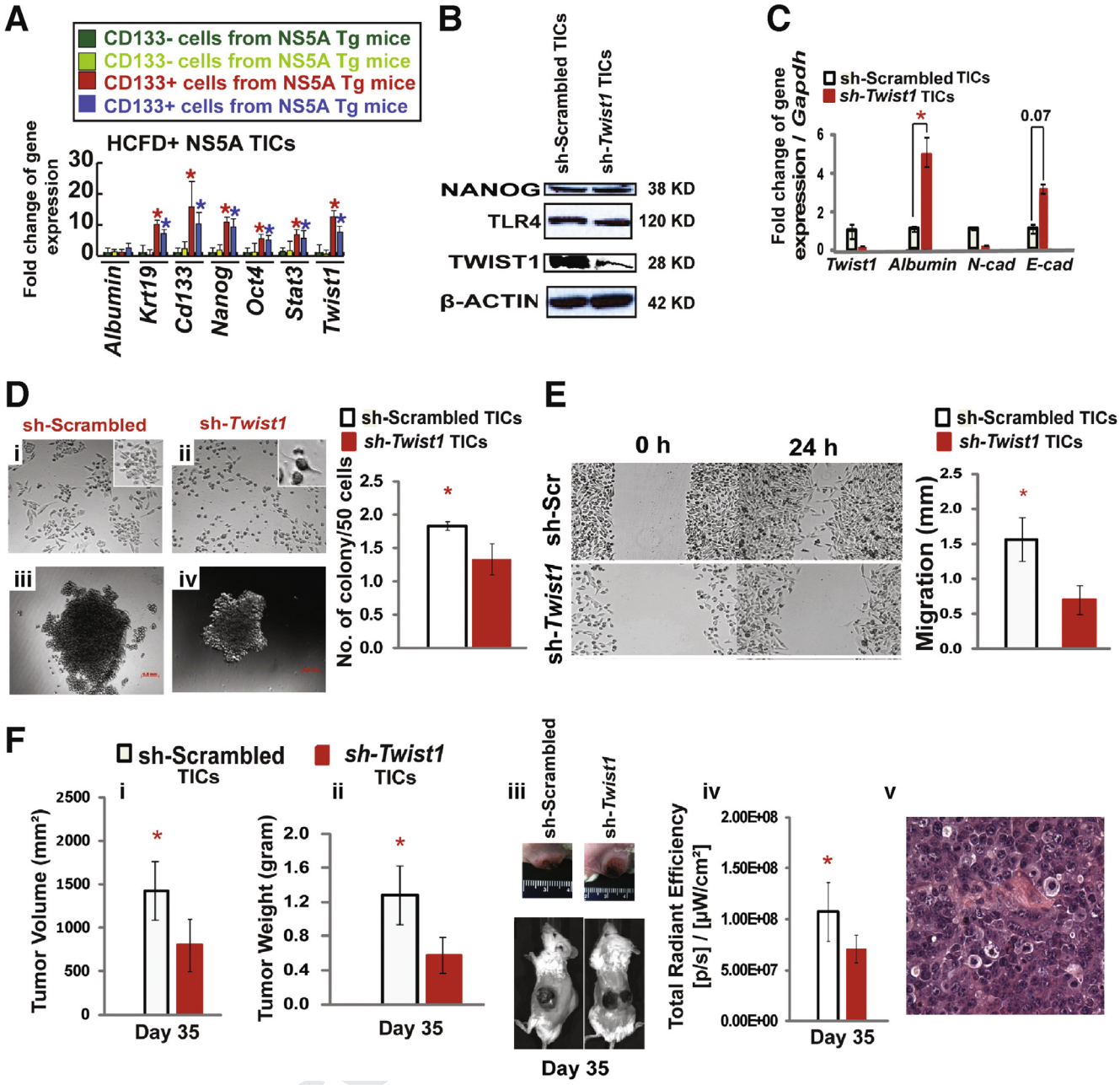

Figure 3. *Twist1* is required for mesenchymal morphology of TICs, down-regulation of *Twist1* reduces TIC cancer-initiating property. (*A*) CD133+/CD49f+/CD45- cells were isolated from tumors of 2 different HCFD-fed *NS5A* Tg mice and examined for stemness gene expression by quantitative real-time PCR. (*B*) To silence *Twist1* expression, lentivirus shRNA *Twist1* was transduced in TICs. Immunoblot analysis confirmed decreased TWIST1 expression in TICs and showed unchanged expression of NANOG and TLR4 (n = 3). (*C*) mRNA levels were validated by quantitative real-time PCR. Expression profile of EMT-regulated genes, including mesenchymal markers (*Twist1* and *N-cad*) and epithelial markers (*albumin* and *E-cadherin*) were analyzed (n = 3; *$P < .05$). (*D*) Light-field microscopy showed an altered morphology of TICs after *Twist1* knockdown. Scrambled TIC (1) parenchymal cell phenotype drastically changed to a tadpole shape (2) after *Twist1* knockdown (40×; n = 10; *insets* are enlarged images). In vitro oncogenicity was tested via soft agar colony formation assay. Silencing *Twist1* in TICs (4) significantly reduced colony-forming ability in contrast to control cells (3). The number of colonies formed was normalized and summarized (n = 3; *$P < .05$). (*E*) shRNA knock down of *Twist1* diminished the ability of TICs to effectively migrate in contrast to the scrambled shRNA control, as shown by in vitro cell migration assay. The images were captured at 0 hours and 24 hours after scratching the cell layer with a 100 μL pipet tip (n = 3; *$P < .05$). (*F*) Analyses at day 35 after TIC transplantation (subcutaneously injected into NOG mice). *Twist1* silencing reduced the overall tumor volume (1) and weight (2). (3) Gross image of subcutaneous tumors. (4) Noninvasive bioluminescence imaging shows the decrease in overall tumor growth (n = 4 NOG mice/cohort; *$P < .05$). (5) H&E staining of xenografted tumor in NOG mice shows HCC histology. *Scale bar*: 50 μm. cad, cadherin; Gapdh, glyceraldehyde-3-phosphate dehydrogenase.

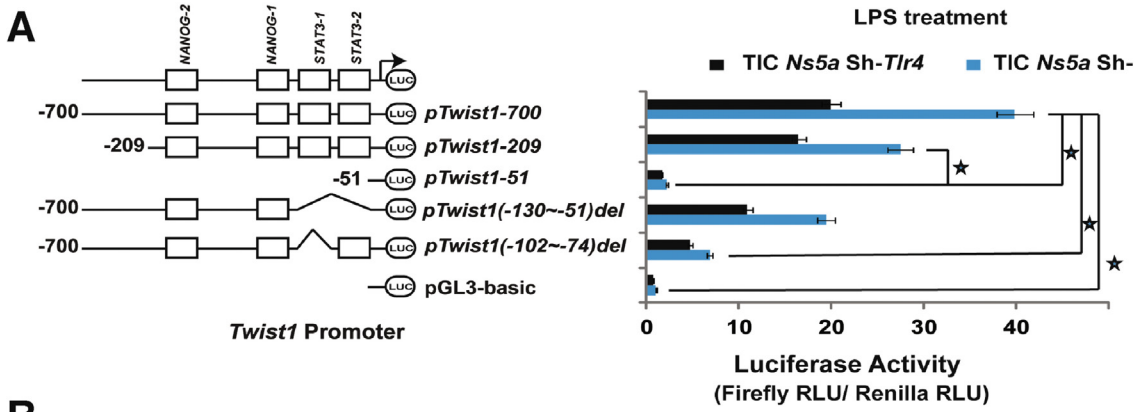

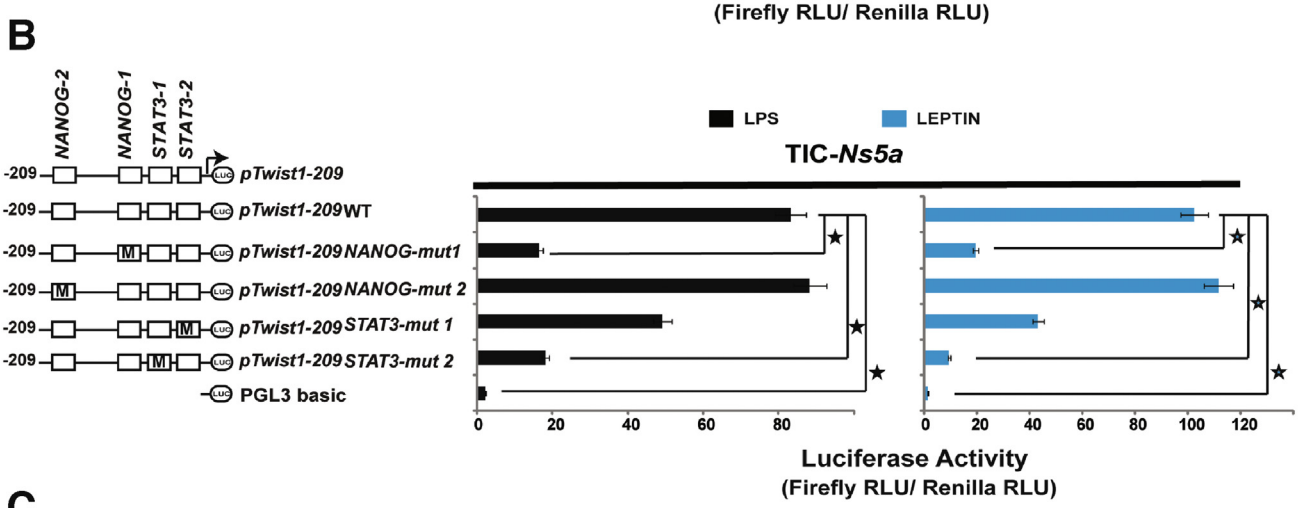

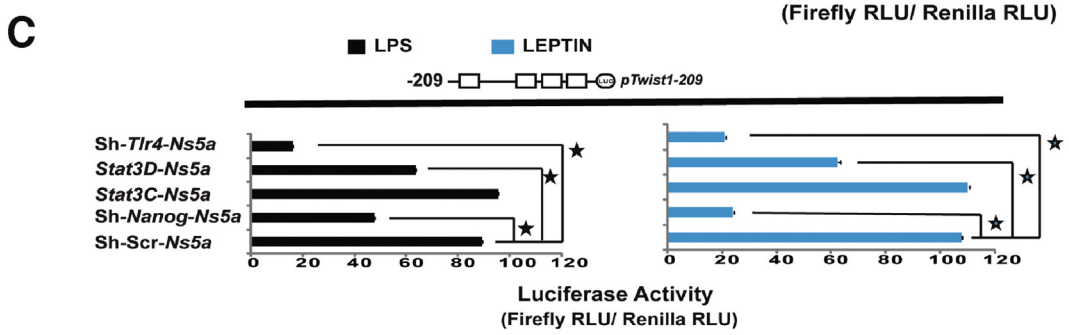

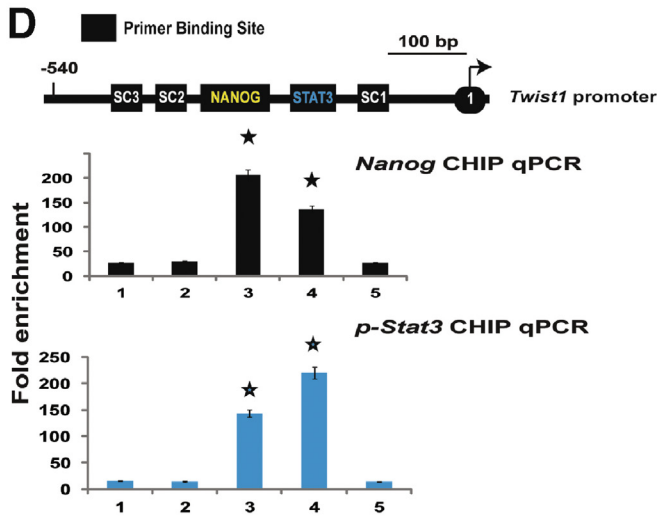

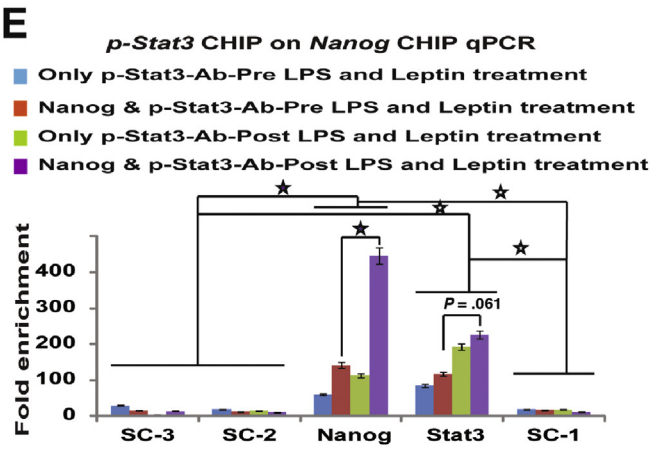

essential cis-elements. Long-term treatment of mice with HCFD activated *Tlr4–Nanog* signaling and increased leptin and endotoxin levels in the plasma. Furthermore, we previously showed that leptin and its receptor (OB-R) augmented pSTAT3 in TICs.[16] In addition, NANOG is known to cooperate with STAT3 for maintenance of pluripotency in mouse embryonic stem cells.[27] Thus, we reasoned for activation of *Twist1* in TICs, the adipose tissue–derived leptin–pSTAT3 signal and the TLR4–NANOG signal are needed. In silico analysis using Transcription Element Search System and Transfac identified consensus NANOG and STAT3 binding sites on the *Twist1* promoter region. To evaluate the functions of these transcription factors, we mutated (Figure 4*B*) the respective NANOG and STAT3 binding sites in the corresponding luciferase reporter construct and discovered that the STAT3-1 (STAT3 site distal to TSS) and NANOG-1 (NANOG site proximal to TSS) sites were critical for *Twist1* promoter activity. As shown in Figure 4*B*, mutations on these specific binding sites markedly attenuated reporter responsiveness to both LPS and leptin induction. In addition, when key upstream cellular signals (*Tlr4*, *Nanog*, and *Stat3*) were blocked, *Twist1* promoter activity was abrogated significantly (Figure 4*C*). This result was substantiated further after chromatin immunoprecipitation (ChIP)–quantitative PCR analysis with antibodies specific for NANOG and pSTAT3 (Figure 4*D*). Single antibody immunoprecipitation of either NANOG or pSTAT3 enriched the NANOG-1 and STAT3-1 binding sites in quantitative PCR, signifying that these 2 transcription factors might cooperatively transactivate *Twist1* in response to LPS and leptin. As further validation of this model, sequential ChIP analysis was performed. As shown in Figure 4*E*, NANOG and pSTAT3 mutually bound each other in the process of transactivating *Twist1*.

Mouse and Human HCC Have Accentuated Expression of TLR4, p-STAT3, and TWIST1

The involvement of both LPS–TLR4–NANOG and Lepin–OB-R–pSTAT3 signaling pathways for *Twist1* induction was examined by immunoblotting analysis of lysates from liver tumors isolated from HCFD-fed *NS5A* Tg mice and normal livers of chow-fed mice. As expected, TLR4, STAT3, pSTAT3, and TWIST1 all were up-regulated (Supplementary Figure 6*A*). The mRNA levels of TLR4, STAT3, and TWIST1 also were increased in quantitative real-time PCR analysis (Supplementary Figure 6*B–D*). Furthermore, immunostaining showed co-localization of TWIST1 with pSTAT3 and NANOG, as well as co-localization of pSTAT3 with NANOG in tumor-bearing HCFD and HCFD + LPS NS5A Tg liver specimens (Figure 5 and Supplementary Figure 7), but less co-localization or fewer numbers of CD133+/CD49F+ or AFP+ cells in LFD-fed NS5A Tg or HCFD-fed *Tlr4*-/- NS5A Tg mice (Supplementary Figure 7). The major source of TLR4 in the liver of wild-type mice is from nonparenchymal cells, including Kupffer cells and stellate cells. The TICs derived from mouse models have significant induction of TLR4. As shown in Supplementary Figure 7, the LFD cohort with immunofluorescence staining shows TLR4-positive cells, which are presumably Kupffer cells or stellate cells. However, in HCFD and HCFD + LPS the TLR4-positive cells have NANOG co-expression, indicating that the TLR4 origin is not only from Kupffer cells or stellate cells, but also from the TICs or hepatocytes. This is corroborated further in Supplementary Figure 7 in which co-staining of TWIST1–NANOG and CD133–CD49F is present in HCFD but not in LFD. Nonparenchymal areas of mice fed both HCFD and LFD have TLR4 staining whereas co-staining of TLR4–NANOG or TLR4–AFP are present mainly in the HCFD group but not in the LFD group and in groups of Tlr4-/-NS5A Tg mice. In liver of NS5A Tg mice, both parenchymal (albumin+) and nonparenchymal staining of TLR4 are positive (Supplementary Figure 8), whereas the nonparenchymal area of WT mice fed LFD mainly have positive staining of TLR4 (Supplementary Figure 7), indicating that hepatocytes and TICs of NS5A Tg mice have increased levels of TLR4, which are associated with strong staining patterns of AFP and TWIST1.

We next assessed the clinical relevance of our findings by analyzing the expression of these proteins in patient-derived HCC samples. Immunofluorescence staining detected co-localization of TWIST1 with TLR4, pSTAT3, and NANOG (Figure 6*A* and Supplementary Figure 10). Moreover, paired immunohistochemical analyses of 142 patient samples (116 as a tissue microarray analysis) (Supplementary Figure 9 and Supplementary Table 1) were

Figure 4. NANOG and STAT3 influence *Twist1* promoter activation in NS5A TICs. (*A*) LPS induces *Twist1* promoter activity in TICs. *Twist1* promoter analysis with various deletion constructs showed the importance of the TSS proximal segment (nt –209/–1). Relative light unit (RLU) values were normalized by *Renilla* luciferase activity driven by a constitutively active SV40 promoter (p*Twist1* nts -1 to -700; **P* < .05; color matched; p*Twist1* nts -1 to -209; #*P* < .05; n = 3). (*B*) NANOG and STAT3 activate the *Twist1* promoter. NANOG and STAT3 binding elements in the *Twist1* promoter region (nts -209 to -51) were mutated by in vitro mutagenesis (p*Twist1* 1-209WT; **P* < .05; color matched; n = 3). (*C*) Silencing *Tlr4* and *Nanog* using lentivirus expressing shRNA or *Stat3* and Stat3D (retrovirus expressing dominant-negative Stat3). **P* < .05; color matched; n = 3). (*D*) *Upper panel*: Schematic representation of the *Twist1* promoter region showing the locations probed for the consensus binding sequences for NANOG (yellow script), STAT3 (green lettering), and the specificity control (SC) regions analyzed by ChIP (white script). Immediately below the schematic representation are NANOG ChIP–quantitative PCR (*black bar graphs*) and STAT3 ChIP–quantitative PCR (blue bar graphs) analyses, which showed the enrichment of NANOG and STAT3 in TICs after LPS (10 μg/mL) and leptin (5 ng/mL) treatment. The fold-enrichment values are relative expression values normalized to the IgG controls (SC3; **P* < .05; SC2; $*P* < .05; SC1; #*P* < .05; biological replicates 4; n = 2). (*E*) Protein–protein–DNA interaction shown by sequential ChIP–quantitative PCR indicated that NANOG and STAT3 bind each other on the *Twist1* promoter region in TICs after LPS (10 μg/mL) and leptin (5 μg/mL) treatment. The fold-enrichment values are relative expression values normalized to the IgG controls (SC3, SC2, SC1; **P* < .05; color matched; #*P* < .05; biological replicates 4; n = 2). qPCR, qualitative PCR.

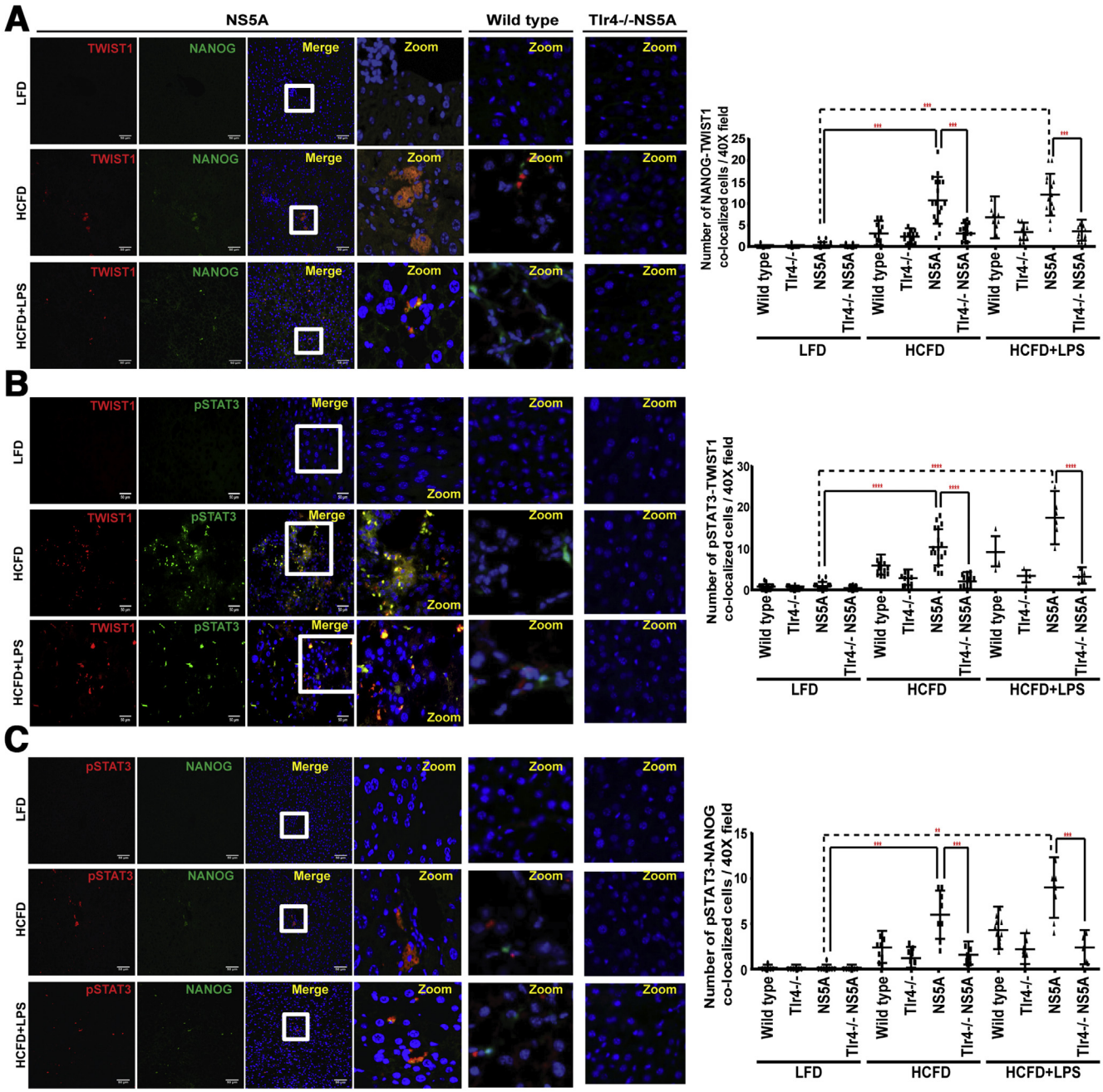

Figure 5. Induction of NANOG, pSTAT3, and TWIST1 in HCFD and HCFD + LPS NS5A Tg cohorts. Confocal immunofluorescence microscopy showed co-localization of TWIST1 with (*A*) NANOG and (*B*) pSTAT3 (C) Co-localization of pSTAT3 with NANOG in tumors obtained from HCFD and HCFD + LPS NS5A Tg liver specimens. This immunoreactivity is completely absent in low-fat diet liver tissues (magnification, 40× oil; n = 15 samples/cohort; n = 3). Quantifications of the immunofluorescence data were performed using Metamorph software. *Scale bar*: 50 μm.

performed to validate the significance of TWIST1 and NANOG in human tissue sections from 3 different cohorts (Figure 6*B* and *C* and Supplementary Figure 9*A*). To corroborate our findings and to gain insights on the correlation of *Twist1* with grade, survival, and relapse in HCC patients, we performed an in silico analysis using the Oncomine Gene browser. Two independent libraries from the repository were analyzed: The Cancer Genome Atlas liver (probing 97 HCC and 59 paired normal liver tissue) and Guichard liver[28] (probing 99 HCC and 86 normal liver). Both showed the significant impact of *TWIST1* on HCC (Figure 6*D* and Supplementary Figure 9*B*).

TWIST1 Overexpression Promotes Tumor Formation

Our results indicated that *Twist1* silencing reduces TIC-derived tumorigenesis (Figure 3*F*) and that *Twist1* is downstream of TLR4 (Figure 4). We then investigated whether overexpression of *Twist1* beyond the basal level in TICs can enhance its role in malignant tumor development

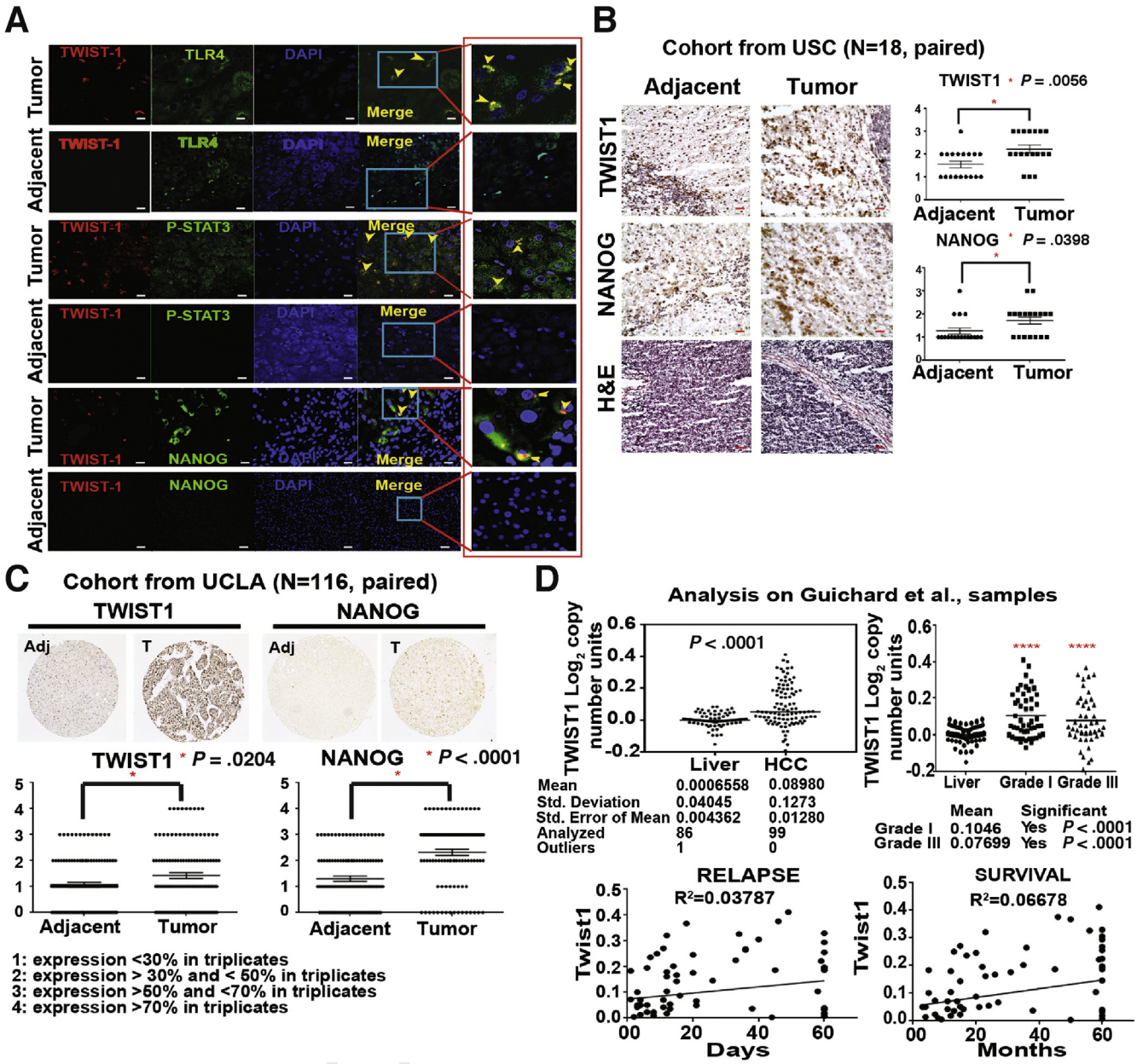

Figure 6. Accentuated TWIST1 co-localization with TLR4, P-STAT3, and NANOG in human patient samples. (*A*) Confocal immunofluorescence imaging studies showed TLR4, P-STAT3, and NANOG often co-localized with TWIST1 in HCC patient liver specimens (tumor), but absent in noncancerous liver tissue (adjacent) (magnification, 40× oil; n = 8 samples/cohort; n = 3; *red boxes* show cropped images). (*B*) Paired IHC staining performed at USC corroborated with immunofluorescence, which showed the significant increase in NANOG and TWIST1 expression in HCC tumor samples (100× magnification; n = 18 samples, paired; n = 3). (*C*) Tissue microarray analysis confirmed the correlation of TWIST1 and NANOG in a large number of patient HCC tumor samples (100× magnification; n = 116 samples, paired). Adjacent, parent noncancerous liver; tumor, human HCC. The liver is removed to transplant new liver. (*D*) In silico analysis using the Oncomine Gene browser, probing for *Twist1* correlation with grade, survival, and relapse in HCC patients via Guichard libraries. *Scale bar*: 50 μm.

and metastasis. In addition, we asked how *Tlr4* silencing can influence this outcome. To test this hypothesis, we transplanted TICs expressing scrambled or *Tlr4* shRNA (Supplementary Figure 11), TICs containing empty vector, or TICs constitutively expressing *Twist1* into NOG recipient mice (Supplementary Figure 11*A*). Overexpression of *Twist1* indeed promoted tumor growth and significantly increased final tumor volume and weight (Figure 7*A* and *B*). Concomitant *Tlr4* silencing (Supplementary Figure 11*B*) reduced the overall tumor volume and weight, indicating that TLR4 acts upstream of *Twist1*. Constitutive overexpression of *Twist1* resulted in increased metastasis to the lung and the liver, suggesting that it has an important role in metastatic progression (Figure 7*C*).

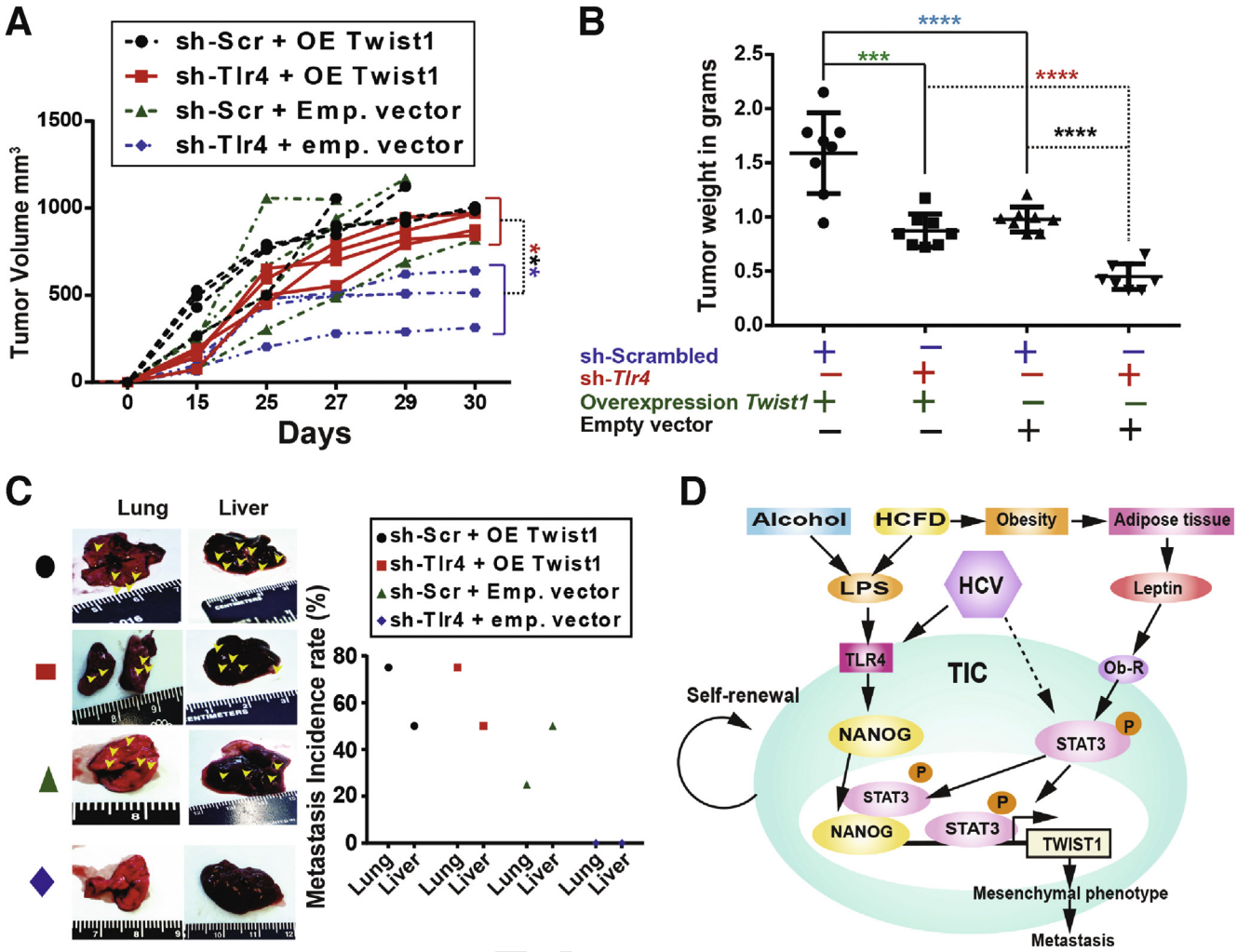

Figure 7. *Twist1* overexpression drives tumor growth independently of *Tlr4*. TICs were transduced with lentivirus expressing shRNA for *Tlr4* or scrambled shRNA followed by a second transduction with retrovirus expressing *Twist1* overexpression (OE) plasmid vector or empty vector (Emp). These cells were injected subcutaneously into the rear flanks of NOG mice (1 million cells/injection). (*A*) Tumor volume measured at days 15, 25, and 30 (also whenever an unexpected death occurred) showed an increasing trend in the tumor volume with intact *Tlr4* and *Twist1* overexpression when compared with their respective controls (sh-Tlr4 + OE vs sh-Tlr4 + Emp; ***$P < .001$; n = 4 NOG mice/cohort; n = 2; statistics performed using 2-way analysis of variance). (*B*) Significant increase in the overall tumor weight (***$P < .001$, ****$P < .0001$, n = 4 *NOG* mice/cohort; n = 2). (*C*) Overexpression of *Twist1* promotes liver and lung metastasis irrespective of the endogenous *Tlr4* expression in TICs. (*D*) A schematic representation of the proposed link between oncogenic TLR4/NANOG signaling, OB-R/pSTAT3, and an effective TWIST1 pathway in generating TICs.

Discussion

TICs comprise a small percentage of cells with stem-like properties resident in tumors and have been documented in a wide variety of cancerous tissues.[29] EMT remodels cells and thus plays a key role in the acquisition of malignant traits.[30,31] In this report, we show that TLR4 is required for liver oncogenesis and the expansion of liver TICs in HCFD-fed HCV–NS5A Tg mice. Analysis of gene expression in TICs showed that *Twist1*, a master regulator of EMT,[17–19] was increased 11-fold, which was not observed in TICs derived from alcohol diet–fed NS5A Tg mice.[14] The findings described an unexpected convergence of the NANOG and STAT3 signaling pathways. We have identified an important functional link between the NANOG pathway, by activation of upstream LPS–TLR4 signaling, and the STAT3 pathway, driven by leptin–OB-R signaling. These 2 pathways cooperate to activate *Twist1* and augment TIC motility (Figure 7*D*).

These studies implicate that lifestyle diseases, including obesity and alcoholism, promote genesis, mesenchymal phenotype, and metastatic characteristics of TICs through synergistic interactions between the LPS–TLR4–NANOG pathway and leptin–Ob-R–STAT3 (Figure 7*D*). Therefore, investigation of the effects of inhibitor combinations to prevent this synergistic interaction, including TLR4 antagonist or inhibitors targeting STAT3, NANOG, and/or TWIST1, is warranted for further investigation in preclinical mouse models.

In conclusion, stemness markers NANOG and STAT3 are activated downstream of the LPS–TLR4 and leptin–OB-R pathways, respectively. NANOG and STAT3 cooperate to drive increased *Twist1* levels, promoting the mesenchymal phenotype and metastasis in TICs (Figure 7*D*) and contributing to HCC development.

Supplementary Material

Note: To access the supplementary material accompanying this article, visit the online version of *Gastroenterology* at www.gastrojournal.org, and at http://dx.doi.org/10.1053/j.gastro.2015.11.002.

References

1. Peters MG, Terrault NA. Alcohol use and hepatitis C. Hepatology 2002;36:S220–S225.
2. Donato F, Gelatti U, Limina RM, et al. Southern Europe as an example of interaction between various environmental factors: a systematic review of the epidemiologic evidence. Oncogene 2006;25:3756–3770.
3. Hassan MM, Hwang LY, Hatten CJ, et al. Risk factors for hepatocellular carcinoma: synergism of alcohol with viral hepatitis and diabetes mellitus. Hepatology 2002;36:1206–1213.
4. Song SJ, Poliseno L, Song MS, et al. MicroRNA-antagonism regulates breast cancer stemness and metastasis via TET-family-dependent chromatin remodeling. Cell 2013;154:311–324.
5. Lai MS, Hsieh MS, Chiu YH, et al. Type 2 diabetes and hepatocellular carcinoma: a cohort study in high prevalence area of hepatitis virus infection. Hepatology 2006;43:1295–1302.
6. Ribeiro PS, Cortez-Pinto H, Sola S, et al. Hepatocyte apoptosis, expression of death receptors, and activation of NF-kappaB in the liver of nonalcoholic and alcoholic steatohepatitis patients. Am J Gastroenterol 2004;99:1708–1717.
7. Feingold KR, Grunfeld C. Role of cytokines in inducing hyperlipidemia. Diabetes 1992;41(Suppl 2):97–101.
8. **Shintani Y, Fujie H**, Miyoshi H, et al. Hepatitis C virus infection and diabetes: direct involvement of the virus in the development of insulin resistance. Gastroenterology 2004;126:840–848. Q32
9. Singh S, Singh PP, Roberts LR, et al. Chemopreventive strategies in hepatocellular carcinoma. Nat Rev Gastroenterol Hepatol 2014;11:45–54.
10. Villanueva A, Hernandez-Gea V, Llovet JM. Medical therapies for hepatocellular carcinoma: a critical view of the evidence. Nat Rev Gastroenterol Hepatol 2013;10:34–42.
11. Gale MJ Jr, Korth MJ, Tang NM, et al. Evidence that hepatitis C virus resistance to interferon is mediated through repression of the PKR protein kinase by the nonstructural 5A protein. Virology 1997;230:217–227.
12. Kato N, Lan KH, Ono-Nita SK, et al. Hepatitis C virus nonstructural region 5A protein is a potent transcriptional activator. J Virol 1997;71:8856–8859.
13. Machida K, Cheng KT, Sung VM, et al. Hepatitis C virus induces toll-like receptor 4 expression, leading to enhanced production of beta interferon and interleukin-6. J Virol 2006;80:866–874.
14. Machida K, Tsukamoto H, Mkrtchyan H, et al. Toll-like receptor 4 mediates synergism between alcohol and HCV in hepatic oncogenesis involving stem cell marker Nanog. Proc Natl Acad Sci U S A 2009;106:1548–1553.
15. Erridge C, Attina T, Spickett CM, et al. A high-fat meal induces low-grade endotoxemia: evidence of a novel mechanism of postprandial inflammation. Am J Clin Nutr 2007;86:1286–1292.
16. Feldman DE, Chen C, Punj V, et al. Pluripotency factor-mediated expression of the leptin receptor (OB-R) links obesity to oncogenesis through tumor-initiating stem cells. Proc Natl Acad Sci U S A 2012;109:829–834.
17. **Mani SA, Guo W, Liao MJ**, et al. The epithelial-mesenchymal transition generates cells with properties of stem cells. Cell 2008;133:704–715.
18. Morel AP, Lievre M, Thomas C, et al. Generation of breast cancer stem cells through epithelial-mesenchymal transition. PLoS One 2008;3:e2888.
19. **Yang J, Mani SA**, Donaher JL, et al. Twist, a master regulator of morphogenesis, plays an essential role in tumor metastasis. Cell 2004;117:927–939.
20. Majumder M, Ghosh AK, Steele R, et al. Hepatitis C virus NS5A protein impairs TNF-mediated hepatic apoptosis, but not by an anti-FAS antibody, in transgenic mice. Virology 2002;294:94–105.
21. Majumder M, Steele R, Ghosh AK, et al. Expression of hepatitis C virus non-structural 5A protein in the liver of transgenic mice. FEBS Lett 2003;555:528–532.
22. Van Heek M, Compton DS, France CF, et al. Diet-induced obese mice develop peripheral, but not central, resistance to leptin. J Clin Invest 1997;99:385–390.
23. Haluzik M, Gavrilova O, LeRoith D. Peroxisome proliferator-activated receptor-alpha deficiency does not alter insulin sensitivity in mice maintained on regular or high-fat diet: hyperinsulinemic-euglycemic clamp studies. Endocrinology 2004;145:1662–1667.
24. Kang Y, Massague J. Epithelial-mesenchymal transitions: twist in development and metastasis. Cell 2004;118:277–279.
25. **Sun T, Zhao N**, Zhao XL, et al. Expression and functional significance of Twist1 in hepatocellular carcinoma: its role in vasculogenic mimicry. Hepatology 2010;51:545–556.
26. **Cheng GZ, Zhang WZ**, Sun M, et al. Twist is transcriptionally induced by activation of STAT3 and mediates STAT3 oncogenic function. J Biol Chem 2008;283:14665–14673.
27. Torres J, Watt FM. Nanog maintains pluripotency of mouse embryonic stem cells by inhibiting NFkappaB and cooperating with Stat3. Nat Cell Biol 2008;10:194–201.
28. Guichard C, Amaddeo G, Imbeaud S, et al. Integrated analysis of somatic mutations and focal copy-number changes identifies key genes and pathways in hepatocellular carcinoma. Nat Genet 2012;44:694–698.
29. Farnie G, Clarke RB. Breast stem cells and cancer. Ernst Schering Found Symp Proc 2006:141–153. Q33

30. Nawshad A, Lagamba D, Polad A, et al. Transforming growth factor-beta signaling during epithelial-mesenchymal transformation: implications for embryogenesis and tumor metastasis. Cells Tissues Organs 2005;179:11–23.
31. Thiery JP. Epithelial-mesenchymal transitions in development and pathologies. Curr Opin Cell Biol 2003; 15:740–746.

Author names in bold designate shared co-first authorship.

Received June 2, 2015. Accepted November 1, 2015.

Reprint requests
Address requests for reprints to: Keigo Machida, PhD, Department of Molecular Microbiology and Immunology, University of Southern California, Keck School of Medicine, 2011 Zonal Avenue, HMR503C, Los Angeles, California. e-mail: keigo.machida@med.usc.edu; fax: (323) 442-1721.

Acknowledgments
The authors thank Dr Ratna Ray (Saint Louis University) for providing HCV *NS5A* Tg mice; Professor Stanley M. Tahara, Mr Chad Nakagawa, and Mrs Kelly Brewer (University of Connecticut Health) for critical reading of the manuscript; Professor Hidekasu Tsukamoto (USC) and Professor Si-Yi Chen (USC) for discussion; Professor Susan Groshen and Ms Lingyun Ji, of the USC Norris Comprehensive Cancer Center Biostatistics Core supported by NIH/NCI P30 CA 014089 for statistical analyses; USC Molecular Imaging Center supported by NIH/NVRR S10 for animal imaging; Ms Lewei Duan for technical assistance; and Mr Yibu Chen and Ms Meng Li Dual in the Norris Medical Library supported bioinformatics analyses. The TWIST1-pGL3 reporter constructs were obtained from Dr Nakamura (Tokyo Medical and Dental University, Japan). Retroviruses expressing *Stat3C* and *Stat3D* were obtained from Professor Daniel C. Link (Washington University of School of Medicine).

The data used in this study have been deposited in NCBI under GSE61435 (Microarray).

Dinesh Babu Uthaya Kumar, Keigo Machida, and Douglas Feldman conceived the study; Dinesh Babu Uthaya Kumar, Chia-Lin Chen, Jian-Chang Liu, Keigo Machida, Joseph DiNorcia, Bita Naini, Sunhawit Junrungsee, Samuel French, Samuel W. French, Vatche Garen Agopian, and Ali Zarrinpar obtained the data; Dinesh Babu Uthaya Kumar, Chia-Lin Chen, Keigo Machida, Jian-Chang Liu, Joseph DiNorcia, Bita Naini, Sunhawit Junrungsee, Samuel French, Samuel W. French, Vatche Garen Agopian, and Ali Zarrinpar provided data management and statistical support; and Dinesh Babu Uthaya Kumar, Jian-Chang Liu, and Keigo Machida conducted the data analysis and drafted the report. All authors interpreted the data and contributed to the final version of this report.

Conflicts of interest
The authors disclose no conflicts.

Funding
Supported by National Institutes of Health research grants R01AA018857 and P50AA011999 (Southern California Research Center for ALPD and Cirrhosis, pilot project, program, animal core, morphology core); Lee Summer Project funding P30DK048522 (USC Research Center for Liver Diseases, pilot project program); the Non-Parenchymal Liver Cell Core (R24AA012885); and UO-021898. This research also was supported by a Research Scholar Grant (RSG-12-177-01-MPC); pilot funding from the American Cancer Society (IRG-58-007-48); the Cell and Tissue Imaging Core–USC Research Center for Liver Diseases (P30 DK048522).